# Stereoselective olefin cyclopropanation under aerobic conditions with an artificial enzyme incorporating an iron-chlorin e6 cofactor.

Gopeekrishnan Sreenilayam, Eric J. Moore, Viktoria Steck, and Rudi Fasan\*

Department of Chemistry, University of Rochester, Rochester NY 14627, United States

ABSTRACT: Myoglobin has recently emerged as a promising biocatalyst for catalyzing carbene-mediated cyclopropanation, a synthetically valuable transformation not found in nature. Having naturally evolved for binding dioxygen, the carbene transferase activity of this metalloprotein is severely inhibited by it, imposing the need for strictly anaerobic conditions to conduct these reactions. In this report, we describe how substitution of the native heme cofactor with an iron-chlorin e6 complex enabled the development of a biocatalyst capable of promoting the cyclopropanation of vinylarenes with high catalytic efficiency (up to 6,970 TON), turnover rate (>2,000 turnovers/min), and stereoselectivity (up to 99% de and ee) in the presence of oxygen. The artificial metalloenzyme can be recombinantly expressed in bacterial cells, enabling its application also in the context of whole-cell biotransformations. This work makes available a robust and easy-to-use oxygen-tolerant biocatalyst for asymmetric cyclopropanations and demonstrates the value of porphyrin ligand substitution as a strategy for tuning and enhancing the catalytic properties of hemoproteins in the context of abiological reactions.

Keywords: cyclopropanation; myoglobin; artificial metalloenzyme; chlorin e6; biocatalysis

Chiral cyclopropanes constitute highly valuable building blocks in medicinal chemistry, providing key pharmacophores in several drug molecules such as the antidepressant Tranyleypromine<sup>1</sup> and the platelet aggregation inhibitor Ticagrelor<sup>2</sup>, among others.3 Major progress has been made in the development of synthetic methods to access these important structural motifs, including those relying on the transition-metal catalyzed addition of a carbenoid species to the carbon-carbon bond of an olefin.<sup>4</sup> Over the past few years, biocatalytic strategies for promoting olefin cyclopropanation reactions have also emerged, involving engineered variants of heme-containing proteins such as cytochrome P450s<sup>5</sup> and myoglobins (Mb)<sup>6</sup> or other proteins scaffolds.<sup>7</sup> In particular, our group has previously shown how engineered myoglobins can provide promising catalysts for asymmetric cyclopropanation reactions<sup>6</sup> and other carbene-mediated transformations.8

Myoglobin-catalyzed olefin cyclopropanation in the presence of diazo compounds is assumed to be mediated by a heme-carbenoid complex generated upon reaction of the carbene donor reagent with the protein-bound heme cofactor. <sup>6a</sup> Previous studies established that reduction of the hemoprotein to its ferrous state is critical for supporting cyclopropanation activity. <sup>6a</sup> Since ferrous myoglobin has high affinity for oxygen, this non-native reactivity is severely

suppressed in the presence of air, imposing the need for strictly anaerobic conditions to realize these transformations. While this inhibitory effect is somewhat alleviated by mutations at the level of the distal histidine residue,9 which is directly involved in stabilizing the oxy-form of myoglobin, <sup>10</sup> the catalytic activity of Mb-based cyclopropanation catalysts is drastically reduced in the presence of oxygen. A similar drawback concerns iron-porphyrins and other synthetic ironbased catalysts previously investigated for cyclopropanation reactions.<sup>11</sup> These limitations have prompted us to investigate strategies for overcoming the oxygen intolerance of these carbene transfer biocatalysts, a goal that would greatly simplify the application of these systems in organic synthesis. Herein, we report the development of a highly efficient and stereoselective myoglobin-based catalyst for promoting asymmetric olefin cyclopropanations under aerobic conditions.

The native cofactor of myoglobin is iron-protoporphyrin IX (hemin), which is embedded in a hydrophobic pocket of the protein and bound via coordination of the iron atom by a conserved 'proximal' histidine residue (His93 in sperm whale Mb). 10a We and others recently showed how substitution of the metal center in this cofactor can provide a means to alter the reactivity of myoglobin in carbene and nitrene transfer reactions. 9,12 We reasoned that substitution of the porphyrin ligand could provide an alternative approach for tuning the electronic properties of the metal center and thus the reactivity of these biocatalysts, including their susceptibility to oxygen inhibition. With this idea in mind, we focused our attention on chlorin e6 (Ce6), a derivative of the tetrapyrrole chromophore of chlorophyll. Compared to protoporphyrin IX, Ce6 (1) contains a partially saturated pyrrole group (ring D, Figure 1a) and three carboxylic groups, one of which is directly linked to the pyrrole ring C (instead of two propionic groups connected to rings C and D). These structural differences were expected to make Ce6 a more electrondeficient ligand than ppIX, possibly increasing the electrophilicity and thus the reactivity of the putative iron-carbene intermediate<sup>6a,13</sup> implicated in hemoprotein-catalyzed carbene transfer reactions. In addition, the introduction of electronwithdrawing groups in heme analogs was previously reported to reduce their relative affinity for oxygen, 14 suggesting that a similar effect could be obtained with the more readily available Ce6 ligand. Previous investigation of metallated chlorin e6 complexes have been limited to Mg(II)<sup>15</sup> and Zn(II) complexes, the latter being involved in electron transfer processes as part of artificial photosynthetic systems. 16

To prepare the desired iron-Ce6 complex (2), commercially available Ce6 was refluxed with excess Fe(II) chloride tetrahydrate (FeCl<sub>2</sub>.4H<sub>2</sub>O) and L-ascorbic acid in acetone, resulting in the isolation of [Fe(Cl)(Ce6)] (2) as a dark green compound in 96% yield (Figure 1a). The iron complex shows a strong absorbance in the 390-400 nm range of the visible spectrum, corresponding to the Soret band (Figure 1b). Despite the structural differences between hemin and iron-chlorin e6 (2), inspection of the crystal structure of Mb suggested the steric feasibility of accommodating the non-native cofactor into the Mb scaffold (Figure S1). Indeed, the C and D rings of the complex 2 and the 'extra' acetyl group at the C15 meso position were expected to occupy the solvent-exposed side of the heme pocket. In addition, heme analogs carrying bulky groups appended to the propionate group(s) have been successfully introduced into the myoglobin scaffold.<sup>17</sup> Experimentally, we found that iron-chlorin e6 (2) could be readily incorporated into the hemin-free form of wildtype sperm whale myoglobin (apoMb) to give the desired cofactor-substituted metalloprotein (Mb[Fe(Ce6)]). Most conveniently, this process was carried out by adapting a protocol introduced by Watanabe and coworkers, 18 in which E. coli cells expressing apoMb are lysed in the presence of 2, followed by purification of the reconstituted metalloprotein via Ni-affinity chromatography (yield: 2.5 mg protein/L culture). Upon incorporation into the Mb protein scaffold, the Soret band of the cofactor undergoes a redshift ( $\lambda_{max}$ : 395  $\rightarrow$  413 nm) and increase in intensity ( $\epsilon_{413}$  = 188,130 M<sup>-1</sup> cm<sup>-1</sup> vs.  $\varepsilon_{395} = 33,840$  M<sup>-1</sup> cm<sup>-1</sup>; **Figure 1b**). As observed for proteins containing metallochlorin cofactors, 19 Mb[Fe(Ce6)] exhibits a green color as opposed to the characteristic red color of Mb (Figure 1c), further evidencing the different electronic properties of the non-native cofactor compared to hemin.

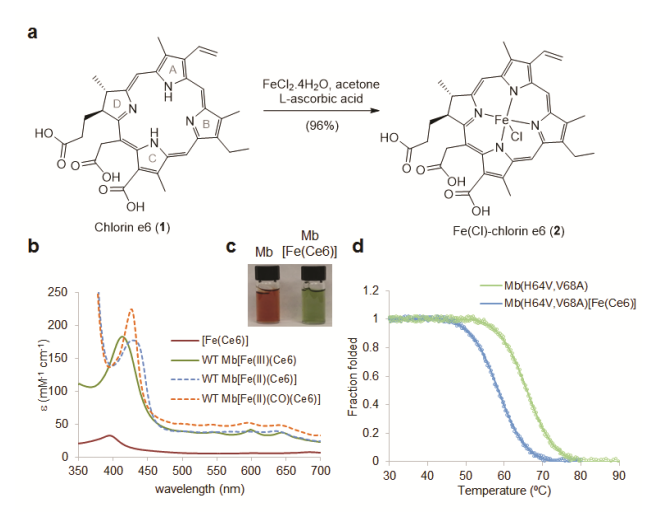


Figure 1. Iron-chlorin e6-substituted myoglobins. (a) Synthesis of Fe(Cl)-chorin e6 complex ([Fe(Ce6)]). (b) Overlay of the absorption spectra for [Fe(Ce6)], and Mb[Fe(Ce6)] in its ferric, ferrous, and CO-bound state. (c) Solutions of Mb and Mb[Fe(Ce6)]. (d) Thermal denaturation curves for Mb(H64V,V68A) and Mb(H64V,V68A)[Fe(Ce6)] as determined by circular dichroism ( $\theta_{222}$ ). See also **Figure S4**.

Building upon these results, we prepared a Fe(Ce6)-containing variant of Mb(H64V,V68A), which we previously

identified as a highly active and stereoselective catalyst for olefin cyclopropanation. 6a The Mb(H64V,V68A) scaffold was expected to provide a model system to both examine the relative performance of the non-native cofactor ([Fe(Ce6)]) versus the heme group within the protein matrix and evaluate the impact of cofactor substitution on the stereoselectivity of the metalloprotein. In initial experiments, the effect of [Fe(Ce6)] incorporation on the structure and stability of Mb(H64V,V68A) was investigated by circular dichroism (CD). The far UV CD spectrum of Mb(H64V,V68A)[Fe(Ce6)] was found to exhibit a profile similar to that of the heme-containing counterpart (Figure S2), indicating the lack of major perturbations in the secondary structure of the protein upon incorporation of the non-native cofactor. Thermal denaturation experiments further revealed Mb(H64V,V68A)[Fe(Ce6)] has reduced stability compared to Mb(H64V,V68A) ( $\Delta T_m = -7.6$ °C) (Figure 1d and S4). This difference notwithstanding, the apparent melting temperature (T<sub>m</sub>) of the artificial metalloprotein (58.4°C) remains comparable or higher than that of heme-dependent enzymes from mesophilic organisms  $(T_m \sim 45-55^{\circ}C)^{21}$ .

To examine the cyclopropanation activity of the Fe(Ce6)-based Mb variants, initial reactions were carried out using styrene (3) as the substrate and ethyl α-diazoacetate (4, EDA) as the carbene donor under 'standard reaction conditions' (0.01 M olefin, 0.02 M EDA, 0.01 M Na<sub>2</sub>S<sub>2</sub>O<sub>4</sub>, 0.1 mol% catalyst). Under anaerobic conditions, Mb[Fe(Ce6)] produced (*E*)-ethyl-2-phenylcyclopropane-1-carboxylate (5) in low yield (16%; 160 catalytic turnovers (TON)) and enantioselectivity (82% *de*, -20% *ee*). Comparable yields (15%; 150 TON) but lower diastereoselectivity (69% *de*) and no enantioselectivity were obtained in parallel reactions with the cofactor alone (Fe(Ce6)). In stark contrast to the poor activity of the wild-type Mb-derived variant, the reaction with Mb(H64,V64)[Fe(Ce6)] furnished quantitative yields of 5 along with excellent diastereo- and enantioselectivity

**Table 1.** Catalytic activity and stereoselectivity of Fe(Ce6)- and heme-containing Mb variants in styrene cyclopropanation with EDA under aerobic conditions. Standard reaction conditions: 10 mM styrene, 20 mM EDA, 10 mM Na<sub>2</sub>S<sub>2</sub>O<sub>4</sub>, 10  $\mu$ M catalyst in KPi buffer (pH 7), room temperature.

Entry	Protein	Cofactor	Yielda	TON	de <sup>b</sup>	ee b
1	-	Fe(Ce6)	1%	14	63%	-5%
2	Mb	Fe(Ce6)	6%	57	77%	22%
3	Mb(H64V,V68A)	Fe(ppIX)	43%	434	98%	95%
4	Mb(H64V,V68A)	Fe(Ce6)	>99%	>990	99.6%	98%
5	Mb(H64V,V68A)	Fe(Ce6)	>99% <sup>c</sup>	>990	99.8%	99%
6	Mb(H64V,V68A,H93F)	Fe(Ce6)	22%	222	52%	12%
7	Mb(H64V,V68A,H93A)	Fe(Ce6)	9%	90	73%	19%
8	Mb(H64V,V68A)	Fe(ppIX)	<1% <sup>d</sup>	<5	-	-
9	Mb(H64V,V68A)	Fe(Ce6)	57% <sup>d</sup>	572	95%	92%
10	Mb(H64V,V68A)	Fe(Ce6)	70% <sup>e</sup>	1,390	99.7%	98%
11	Mb(H64V,V68A)	Fe(Ce6)	35% <sup>f</sup>	6,970	99.6%	99%

 $^a$  Based on GC conversion using calibration curves with isolated **5**. Error is within 15%  $^b$  For trans-(15,25) stereoisomer as determined with chiral GC.  $^c$  Reaction time: 5 min.  $^d$  No reductant (Na<sub>2</sub>S<sub>2</sub>O<sub>4</sub>) added to reaction.  $^e$  With 20 mM styrene, 40 mM EDA.  $^f$  With 1  $\mu$ M Mb variant, 20 mM styrene, 40 mM EDA.

(99.6% de; 98.5% ee). Such catalytic activity and stereoselectivity compare well with those of Mb(H64V,V68A), indicating that (a) the iron-chlorin cofactor is catalytically competent toward carbene transfer and (b) the stereoinductive effect provided by the two active site mutations could be transferred to the [Fe(Ce6)]-based biocatalyst.

To evaluate the ligand effect on the oxygen sensitivity of these biocatalysts, the same reaction was then carried out under aerobic conditions (i.e., in open vessel reactions). In agreement with previous observations,9 the presence of oxygen significantly reduces the catalytic activity of Mb(H64V,V68A), which exhibits only ~430 TON for the formation of 5 (Entry 3, Table 1) compared to >10,000 TON<sup>6a</sup> under oxygen-free conditions. The stereoselectivity of the transformation is also affected (98% de and 95% ee vs. >99.9% de and ee). In stark contrast, the reaction with Mb(H64V,V68A)[Fe(Ce6)] afforded the cyclopropanation product 5 in quantitative yields and excellent diastereomeric and enantiomeric excess (99.6% de; 98% ee) also in the presence of oxygen (Entry 4). Product yields remained high (70%) even after reducing the catalyst loading to 0.05 mol% (Entry 10). The Mb(H64V,V68A)[Fe(Ce6)]-catalyzed reactions proceed cleanly, i.e. without formation of carbene dimerization byproducts (i.e., diethyl maleate/fumarate), even upon single addition of the diazo reagent to the reaction mixture. Time-course experiments showed Mb(H64V,V68A)[Fe(Ce6)] is also a remarkably fast catalyst, featuring an initial product formation rate of over 2,000 turnovers per minute and enabling the reaction to reach completion within five minutes (Entry 5, Table 1). The Mb(H64V,V68A)[Fe(Ce6)]-catalyzed cyclopropanation of styrene with EDA follows Michaelis-Menten kinetics (Figure S5) and from the corresponding curves an apparent K<sub>M(EDA)</sub> of 32 mM and apparent k<sub>cat</sub> of 2,840 min<sup>-1</sup> was estimated.<sup>22</sup> These parameters correspond to a catalytic efficiency ( $k_{cat}/K_{\rm M}$ ) of 1.4 x 10<sup>3</sup> M<sup>-1</sup>s<sup>-1</sup>, which falls within the range of  $k_{\text{cat}}/K_{\text{M}}$  values (10<sup>3</sup>-10<sup>6</sup> M<sup>-1</sup>s<sup>-1</sup>) observed for the majority (60%) of naturally occurring enzymes.<sup>23</sup> For the same reaction, Mb(H64V,V68A) exhibits a comparable K<sub>M(EDA)</sub> value (41 mM) but a significantly lower turnover number ( $k_{\text{cat}}$ : 545 min-1), likely due to the inhibitory effect of oxygen. The superior performance of the iron-chlorin e6 containing variant became apparent also from its catalytic efficiency in terms of total turnovers. Under catalyst-limited conditions, Mb(H64V,V68A)[Fe(Ce6)] supports over 6,900 total turnovers (TTN) in the styrene cyclopropanation reaction (Entry 11), as opposed to <500 TTN for the heme-containing counterpart. Altogether, these results indicated that the chlorin ligand is able to confer the Mb-based variant with high cyclopropanation reactivity in the presence of oxygen.

Interestingly, Mb(H64V,V68A)[Fe(Ce6)] was found to maintain significant cyclopropanation activity also in the absence of reductant (572 TON, Entry 9). Under identical conditions, negligible product formation is observed with the heme-containing Mb(H64V,V68A) (<5 TON, Entry 8), a result consistent with our previous observations that the ferrous species is the catalytically competent form of the hemoprotein in carbene transfer reactions.<sup>6a</sup> To determine

whether ferrous Mb(H64V,V68A)[Fe(Ce6)] is formed during the reaction, e.g., upon reduction by EDA<sup>11a,11b,24</sup>, the reaction with ferric Mb(H64V,V68A)[Fe(Ce6)] was carried out in the presence of carbon monoxide, which binds and potently inhibits the ferrous but not the ferric form of the protein (Figure 1b). Under these conditions, the cyclopropanation product accumulated in lower but still significant amounts (240 TON), indicating that ferric Mb(H64V,V68A)[Fe(Ce6)] is indeed responsible for at least part of the catalytic activity observed in the absence of reductant. Thus, these results suggest that in addition to providing tolerance toward oxygen inhibition, the chlorin ligand enables the metalloprotein to be catalytically active also in the ferric form. Fe(III)-based catalysts active in cyclopropanation reactions have been documented before, but these systems were characterized by low diastereoselectivity (<2.5:1 for trans:cis) and no stereoselectivity. 11c,25

Incorporation of [Fe(Ce6)] into the protein enhances its cyclopropanation reactivity (Entry 2 vs 1, Table 1) and further enhancements in both activity and stereoselectivity derive from the active site mutations (Entry 4 vs. 2). To gain further insight into structural determinants of activity in Mb(H64V,V68A)[Fe(Ce6)], two variants of this protein were prepared in which the proximal histidine (His93) is mutated to Phe or Ala. The H93F mutation replaces the iron-binding imidazolyl group with an isosteric but non-Lewis basic phenyl group, whereas the H93A substitution creates a cavity at the proximal side of the cofactor, 26 likely favouring metal coordination by a water molecule. Both mutations were found to dramatically reduce the cyclopropanation activity of the Mb variants (Entries 6-7, **Table 1**), indicating that axial ligation of the metal center by the histidine residue is critical for optimal catalytic reactivity.

Next, the substrate scope of the oxygen-tolerant cyclopropanation biocatalyst Mb(H64V,V68A)[Fe(Ce6)] was probed using a range of different vinylarene substrates (6a-17a; Scheme 1). Using this variant, various styrene derivatives including ortho-, meta-, and para-, and di-substituted styrenes could be converted to the desired cyclopropanation products (6b-11b) in excellent yields (>99%) and high diastereo- and enantiomeric excess (93-99% de; 97-99% ee) in open vessel reactions. Notably, both electron-donating (8b, 10b) and electron-withdrawing (9b, 11b) groups in the phenyl ring were well tolerated by the [Fe(Ce6)]-based biocatalyst. α-Methylstyrene (12a) was also converted with high efficiency (90%) and with high diastereo- and enantioselectivity (96% de, 95% ee). Compounds 13a-17a were then tested to explore the scope of the reaction across other types of aryl-substituted olefins. For these substrates, high conversions (70-99%) could be achieved using a two-fold higher catalyst loading (0.2 instead of 0.1 mol%). As an exception, cyclopropanation of 5-vinyl-2,3-dihydrobenzofuran 17a proceeded with high efficiency using our standard reaction conditions. Importantly, high enantio- and diastereoselectivity (93-99% de, 78-96% ee) were achieved in all cases, which further demonstrated the broad substrate scope of the Mb(H64V,V68A)[Fe(Ce6)] catalyst.

**Scheme 1.** Substrate scope of Mb(H64V,V68A)[Fe(Ce6)] in the aerobic cyclopropanation of vinylarenes with EDA. Reaction conditions: 10 mM olefin, 20 mM EDA, 10 mM Na<sub>2</sub>S<sub>2</sub>O<sub>4</sub>, 10  $\mu$ M protein in KPi buffer (pH 7), room temperature. <sup>a</sup> With 20  $\mu$ M protein.

We recently established that a variety of metallosubstituted heme analogs can be incorporated into myoglobin by recombinant means, 9,12a a strategy that bypasses the need vitro reconstitution of these metalloenzymes. 12b Notably, this approach could be readily extended enable the expression to Mb(H64V,V68A)[Fe(Ce6)] in E. coli cells. Interestingly, coexpression of the heterologous heme transporter ChuA<sup>12a</sup> was not required for facilitating the uptake of the non-native [Fe(Ce6)] cofactor by the cells. Following these results, a preparative-scale whole-cell cyclopropanation reaction was carried out using Mb(H64V,V68A)[Fe(Ce6)]-expressing cells in the presence of 0.1 g styrene and a two-fold molar excess of EDA. From this reaction, the cyclopropanation product 5 was isolated in high yield (93%) and stereoselectivity (96% de, 90% ee), thereby demonstrating the scalability of this biocatalytic transformation.

In summary, we have described the development of a highly efficient and stereoselective metalloenzyme for olefin cyclopropanation reactions under aerobic conditions. The oxygen-tolerance, broad substrate scope, and scalability of this biocatalyst support its utility and operational simplicity for asymmetric synthesis. The possibility to produce this artificial enzyme in bacterial cells enabled its application in whole-cell biotransformations and makes it amenable to further optimization via protein engineering and directed evolution. From a catalyst design standpoint, this work provides the first example of a hemoprotein-based carbene transferase incorporating a non-native cofactor other than a proto-

porphyrin IX analog.<sup>9,12b,27</sup> The superior performance of the iron-chlorin containing Mb variant compared to the hemebased counterpart under aerobic conditions highlight the opportunities made available through modification of the metal-coordinating ligand toward modulating the reactivity of these biocatalysts. These studies pave the way to the future investigation of chlorin-based metalloproteins, also in combination with different metals,<sup>9</sup> for obtaining novel and/or improved catalytic properties in the context of olefin cyclopropanation and other synthetically valuable abiological transformations.

#### **ASSOCIATED CONTENT**

#### **Supporting Information**

Supporting information includes detailed description of the experimental procedures, supplementary figures and graphs, and compound characterization data. E.J.M. acknowledges support from the NIH Graduate Training Grant T32GM118283.

#### **AUTHOR INFORMATION**

#### **Corresponding Author**

\* rfasan@ur.rochester.edu

#### **ACKNOWLEDGMENT**

This work was supported in part by the U.S. National Institute of Health grant GM098628 and in part by the U.S. National Science Foundation grant CHE-1609550. MS instrumentation was supported by the U.S. NSF grant CHE-0946653.

#### **REFERENCES**

- (1) Burger, A.; Yost, W. L. J. Am. Chem. Soc. 1948, 70, 2198.
- (2) Springthorpe, B.; Bailey, A.; Barton, P.; Birkinshaw, T. N.; Bonnert, R. V.; Brown, R. C.; Chapman, D.; Dixon, J.; Guile, S. D.; Humphries, R. G.; Hunt, S. F.; Ince, F.; Ingall, A. H.; Kirk, I. P.; Leeson, P. D.; Leff, P.; Lewis, R. J.; Martin, B. P.; McGinnity, D. F.; Mortimore, M. P.; Paine, S. W.; Pairaudeau, G.; Patel, A.; Rigby, A. J.; Riley, R. J.; Teobald, B. J.; Tomlinson, W.; Webborn, P. J. H.; Willis, P. A. *Bioorg. Med. Chem. Lett.* **2007**, *17*, 6013.
  - (3) Talele, T. T. J. Med. Chem. 2016, 59, 8712.
- (4) (a) Doyle, M. P.; Forbes, D. C. Chem. Rev. 1998, 98, 911; (b) Lebel, H.; Marcoux, J. F.; Molinaro, C.; Charette, A. B. Chem. Rev. 2003, 103, 977; (c) Pellissier, H. Tetrahedron 2008, 64, 7041; (d) Lowenthal, R. E.; Abiko, A.; Masamune, S. Tetrahedron Lett. 1990, 31, 6005; (e) Evans, D. A.; Woerpel, K. A.; Hinman, M. M.; Faul, M. M. J. Am. Chem. Soc. 1991, 113, 726; (f) Doyle, M. P.; Winchester, W. R.; Hoorn, J. A. A.; Lynch, V.; Simonsen, S. H.; Ghosh, R. J. Am. Chem. Soc. 1993, 115, 9968; (g) Nishiyama, H.; Itoh, Y.; Matsumoto, H.; Park, S. B.; Itoh, K. J. Am. Chem. Soc. 1994, 116, 2223; (h) Uchida, T.; Irie, R.; Katsuki, T. Synlett 1999, 1163; (i) Che, C. M.; Huang, J. S.; Lee, F. W.; Li, Y.; Lai, T. S.; Kwong, H. L.; Teng, P. F.; Lee, W. S.; Lo, W. C.; Peng, S. M.; Zhou, Z. Y. J. Am. Chem. Soc. 2001, 123, 4119; (j) Huang, L. Y.; Chen, Y.; Gao, G. Y.; Zhang, X. P. J. Org. Chem. 2003, 68, 8179; (k) Fantauzzi, S.; Gallo, E.; Rose, E.; Raoul, N.; Caselli, A.; Issa, S.; Ragaini, F.; Cenini, S. Organometallics 2008, 27, 6143; (1) Carminati, D. M.; Intrieri, D.; Caselli, A.; Le Gac, S.; Boitrel, B.; Toma, L.; Legnani, L.; Gallo, E. Chemistry 2016, 22, 13599.
- (5) (a) Coelho, P. S.; Brustad, E. M.; Kannan, A.; Arnold, F. H. Science 2013, 339, 307; (b) Coelho, P. S.; Wang, Z. J.; Ener, M. E.; Baril, S. A.; Kannan, A.; Arnold, F. H.; Brustad, E. M. Nat. Chem. Biol. 2013, 9, 485; (c) Renata, H.; Wang, Z. J.; Kitto, R. Z.; Arnold, F. H. Catal. Sci. Technol. 2014, 4, 3640; (d) Gober, J. G.; Rydeen, A. E.; Gibson-O'Grady, E. J.; Leuthaeuser, J. B.; Fetrow, J. S.; Brustad, E. M. Chembiochem 2016, 17, 394; (e) Gober, J. G.; Ghodge, S. V.; Bogart, J. W.; Wever, W. J.;

- Watkins, R. R.; Brustad, E. M.; Bowers, A. A. ACS Chem. Biol. 2017, 2, 1726
- (6) (a) Bordeaux, M.; Tyagi, V.; Fasan, R. *Angew. Chem. Int. Ed.* **2015**, *54*, 1744; (b) Bajaj, P.; Sreenilayam, G.; Tyagi, V.; Fasan, R. *Angew. Chem. Int. Ed.* **2016**, *55*, 16110; (c) Tinoco, A.; Steck, V.; Tyagi, V.; Fasan, R. *J. Am. Chem. Soc.* **2017**, *139*, 5293.
- (7) (a) Srivastava, P.; Yang, H.; Ellis-Guardiola, K.; Lewis, J. C. *Nat. Commun.* **2015**, *6*, 7789; (b) Rioz-Martinez, A.; Oelerich, J.; Segaud, N.; Roelfes, G. *Angew. Chem. Int. Ed.* **2016**, *55*, 14136.
- (8) (a) Sreenilayam, G.; Fasan, R. Chem. Commun. 2015, 51, 1532; (b) Tyagi, V.; Bonn, R. B.; Fasan, R. Chem. Sci. 2015, 6, 2488; (c) Tyagi, V.; Fasan, R. Angew. Chem. Int. Ed. 2016, 55, 2512; (d) Tyagi, V.; Sreenilayam, G.; Bajaj, P.; Tinoco, A.; Fasan, R. Angew. Chem. Int. Ed. 2016, 55, 13562.
- (9) Sreenilayam, G.; Moore, E. J.; Steck, V.; Fasan, R. Adv. Synth. Cat. 2017, 359, 2076.
- (10) (a) Phillips, S. E.; Schoenborn, B. P. *Nature* **1981**, *292*, 81; (b) Unno, M.; Chen, H.; Kusama, S.; Shaik, S.; Ikeda-Saito, M. *J. Am. Chem. Soc.* **2007**, *129*, 13394.
- (11) (a) Wolf, J. R.; Hamaker, C. G.; Djukic, J. P.; Kodadek, T.; Woo, L. K. *J. Am. Chem. Soc.* **1995**, *117*, 9194; (b) Lai, T. S.; Chan, F. Y.; So, P. K.; Ma, D. L.; Wong, K. Y.; Che, C. M. *Dalton T.* **2006**, 4845; (c) Edulji, S. K.; Nguyen, S. T. *Organometallics* **2003**, *22*, 3374.
- (12) (a) Bordeaux, M.; Singh, R.; Fasan, R. *Bioorg. Med. Chem.* **2014**, 22, 5697; (b) Key, H. M.; Dydio, P.; Clark, D. S.; Hartwig, J. F. *Nature* **2016**, *534*, 534.
- (13) (a) Khade, R. L.; Zhang, Y. J. Am. Chem. Soc. 2015, 137, 7560;
  (b) Sharon, D. A.; Mallick, D.; Wang, B. J.; Shaik, S. J. Am. Chem. Soc. 2016, 138, 9597.
- (14) Shibata, T.; Nagao, S.; Fukaya, M.; Tai, H. L.; Nagatomo, S.; Morihashi, K.; Matsuo, T.; Hirota, S.; Suzuki, A.; Imai, K.; Yamamoto, Y. *J. Am. Chem. Soc.* **2010**, *132*, 6091.
- (15) Jensen, R. G.; Seely, G. R.; Vernon, L. P. J. Phys. Chem. 1966, 70, 3307.
- (16) (a) Hay, S.; Wallace, B. B.; Smith, T. A.; Ghiggino, K. P.; Wydrzynski, T. *Proc. Natl. Acad. Sci. U.S.A.* **2004**, *101*, 17675; (b) Conlan, B.; Cox, N.; Su, J. H.; Hillier, W.; Messinger, J.; Lubitz, W.; Dutton, P. L.; Wydrzynski, T. *Biochim. Biophys. Acta* **2009**, *1787*, 1112.

- (17) Sato, H.; Hayashi, T.; Ando, T.; Hisaeda, Y.; Ueno, T.; Watanabe, Y. J. Am. Chem. Soc. **2004**, 126, 436.
- (18) Kawakami, N.; Shoji, O.; Watanabe, Y. Chembiochem 2012, 13, 2045.
- (19) (a) Timkovich, R.; Cork, M. S.; Gennis, R. B.; Johnson, P. Y. *J. Am. Chem. Soc.* **1985**, *107*, 6069; (b) Dawson, J. H.; Bracete, A. M.; Huff, A. M.; Kadkhodayan, S.; Zeitler, C. M.; Sono, M.; Chang, C. K.; Loewen, P. C. *FEBS Lett.* **1991**, *295*, 123; (c) Bravo, J.; Verdaguer, N.; Tormo, J.; Betzel, C.; Switala, J.; Loewen, P. C.; Fita, I. *Structure* **1995**, *3*, 401
- (20) Nagai, M.; Nagai, Y.; Aki, Y.; Imai, K.; Wada, Y.; Nagatomo, S.; Yamamoto, Y. *Biochemistry* **2008**, *47*, 517.
- (21) (a) Anzenbacher, P.; Hudecek, J.; Struzinsky, R. *FEBS Lett.* **1982**, *149*, 208; (b) Prieto, G.; Suarez, M. J.; Gonzalez-Perez, A.; Ruso, J. M.; Sarmiento, F. *Phys. Chem. Chem. Phys.* **2004**, *6*, 816.
- (22) Due to the limited solubility of styrene in buffer, the kinetic parameters were determined under sub-saturating concentrations of this co-substrate and thus they should be considered as 'apparent'  $k_{\text{cat}}$  and  $K_{\text{M}}$  values
- (23) Bar-Even, A.; Noor, E.; Savir, Y.; Liebermeister, W.; Davidi, D.; Tawfik, D. S.; Milo, R. *Biochemistry* **2011**, *50*, 4402.
  - (24) Salomon, R. G.; Kochi, J. K. J. Am. Chem. Soc. 1973, 95, 3300.
- (25) Simkhovich, L.; Mahammed, A.; Goldberg, I.; Gross, Z. Chem. Eur. J. 2001, 7, 1041.
- (26) Qin, J.; Perera, R.; Lovelace, L. L.; Dawson, J. H.; Lebioda, L. *Biochemistry* **2006**, *45*, 3170.
- (27) Reynolds, E. W.; McHenry, M. W.; Cannac, F.; Gober, J. G.; Snow, C. D.; Brustad, E. M. *J. Am. Chem. Soc.* **2016**, *138*, 12451.

# Supporting Information for

# Stereoselective olefin cyclopropanation under aerobic conditions with an artificial enzyme incorporating an iron-chlorin e6 cofactor.

Gopeekrishnan Sreenilayam, Eric J. Moore, Viktoria Steck, and Rudi Fasan\*

Department of Chemistry, University of Rochester, 120 Trustee road, Rochester, NY 14627, United States.

#### **Table of contents:**

Figures S1-S5 Page S2-S6

Experimental Procedures Pages S7-S12

Synthetic Procedures Page S13-S19

References Page S20

NMR spectra Pages S21-22

<sup>\*</sup> Corresponding author. Email: rfasan@ur.rochester.edu.

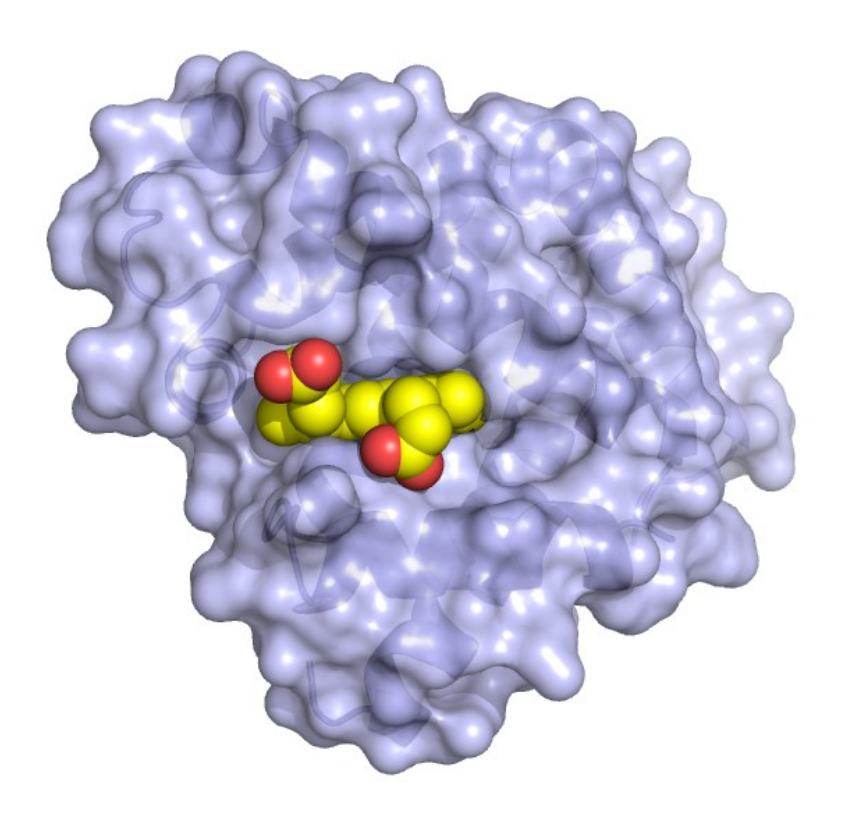
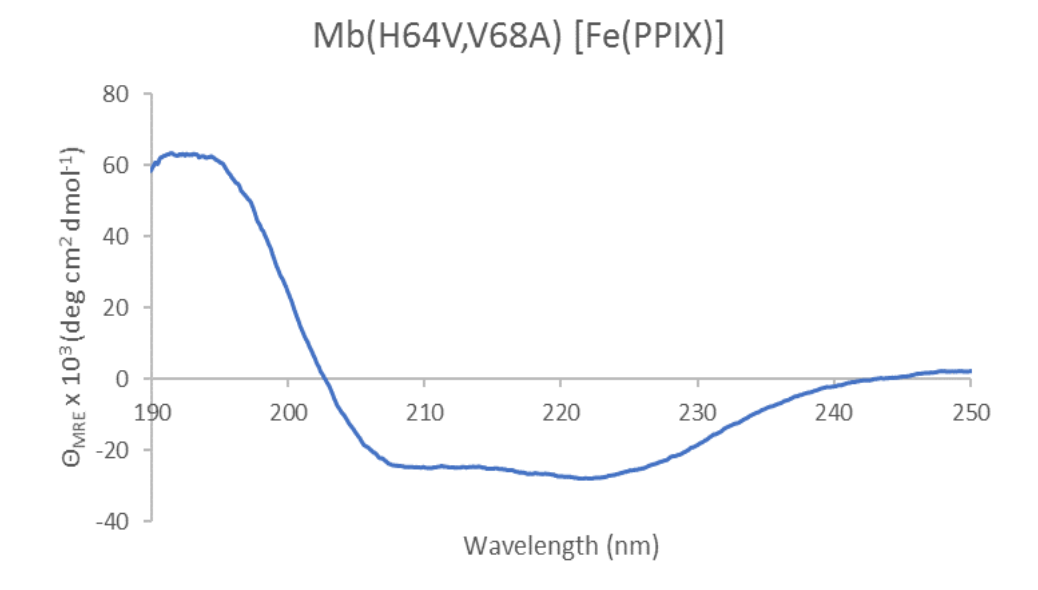


**Figure S1.** Surface representation of the crystal structure of sperm whale myoglobin (PDB 1A6K). The heme cofactor is shown as sphere models (yellow). In the Mb[Fe(Ce6)] complex, the Fe(Ce6) cofactor is expected to adopt an orientation along the C10-C20 axis analogous to that of the heme cofactor in Mb, whereby the propionic, acetyl, and carboxylic group appended to the tetrapyrrole ring are projected toward the solvent.

(a)



(b)

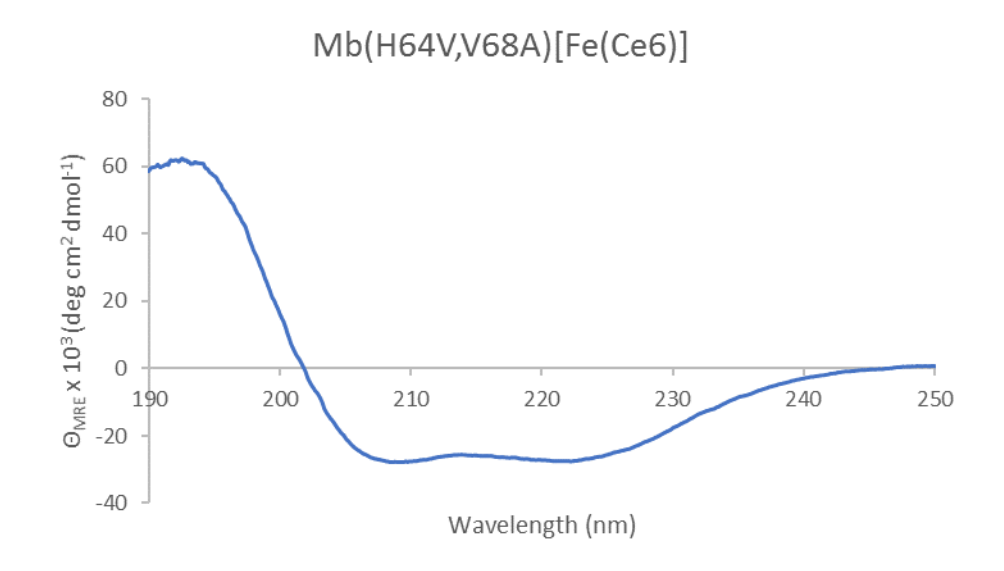
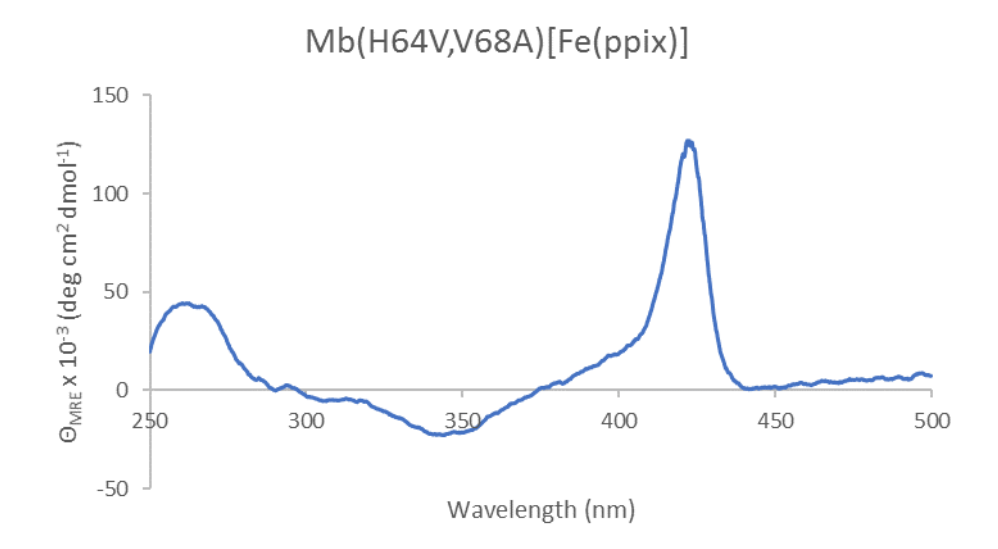


**Figure S2.** UV-range circular dichroism (CD) spectra corresponding to (a) Mb(H64V,V68A) and (b) Mb(H64V,V68A)[Fe(Ce6)].

(a)



(b)

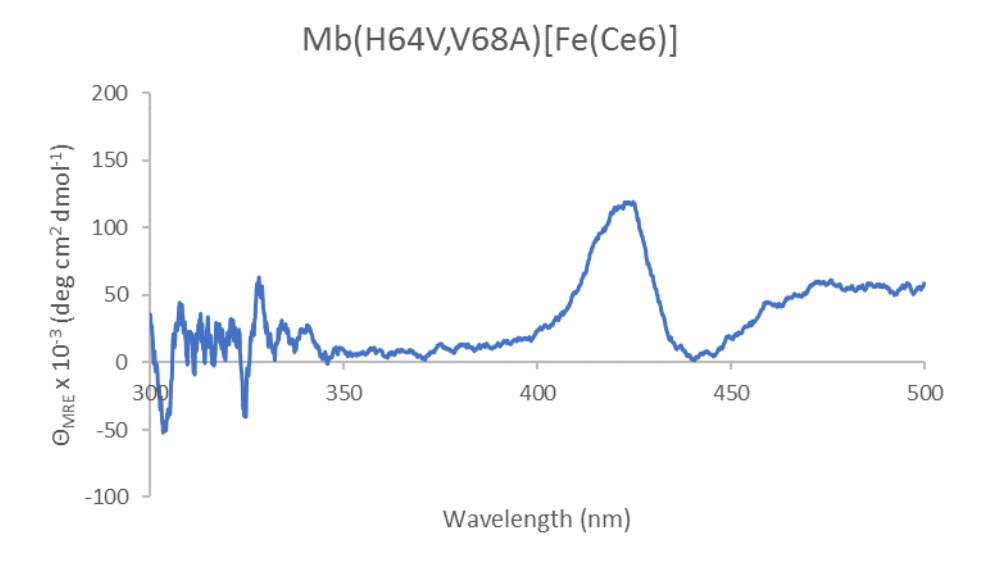
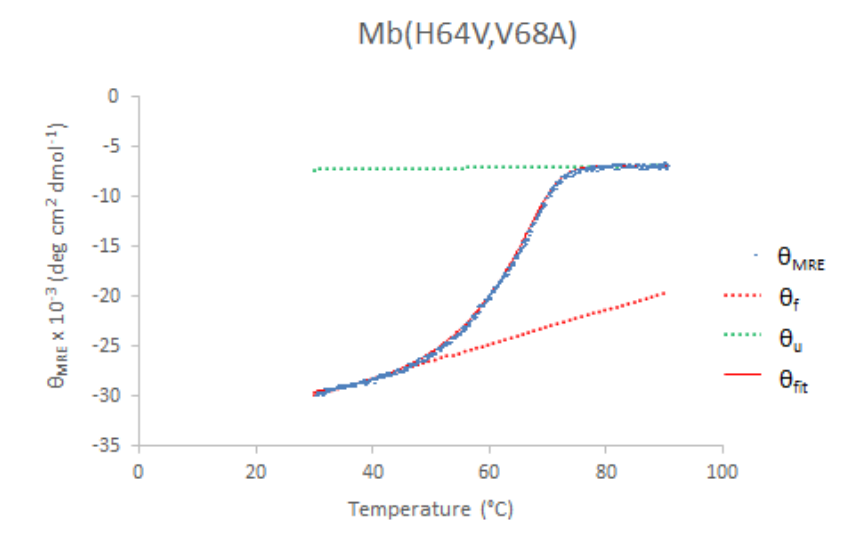


**Figure S3.** Visible-range circular dichroism (CD) spectra corresponding to (a) Mb(H64V,V68A) and (b) Mb(H64V,V68A)[Fe(Ce6)].

(a)



(b)

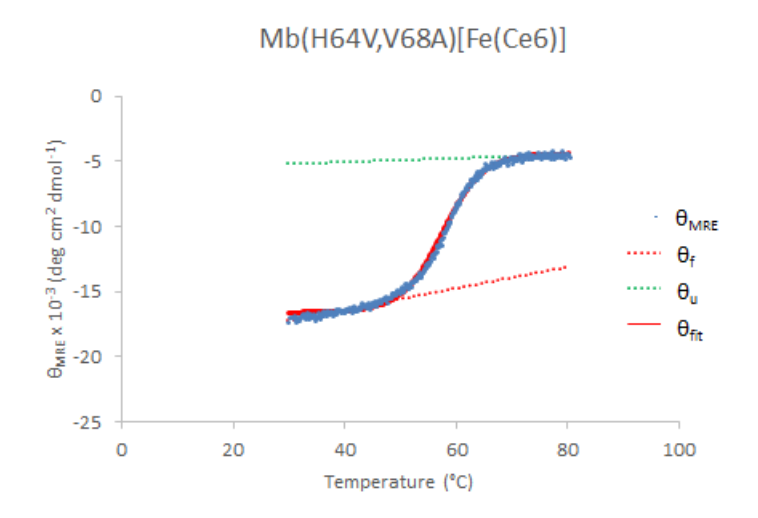
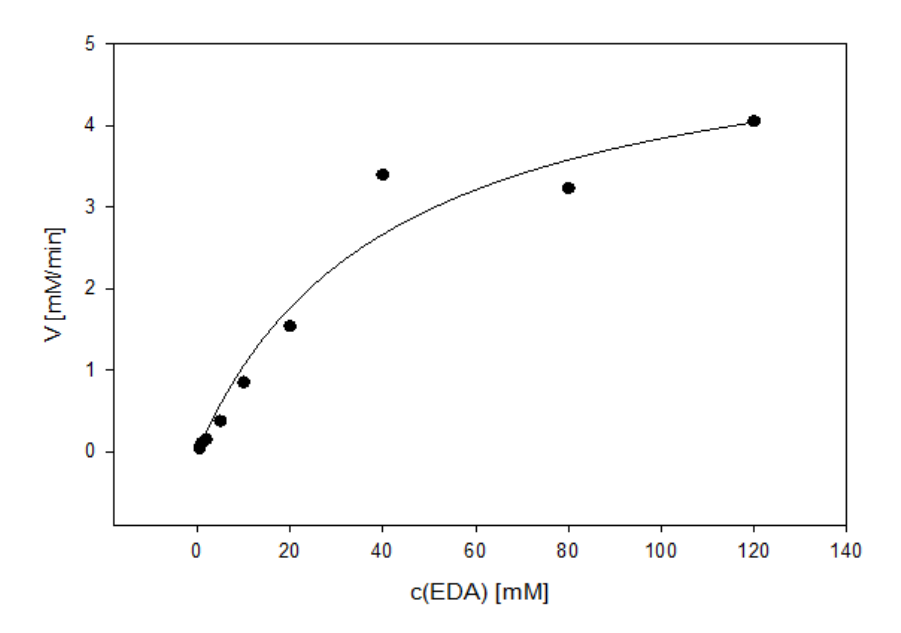
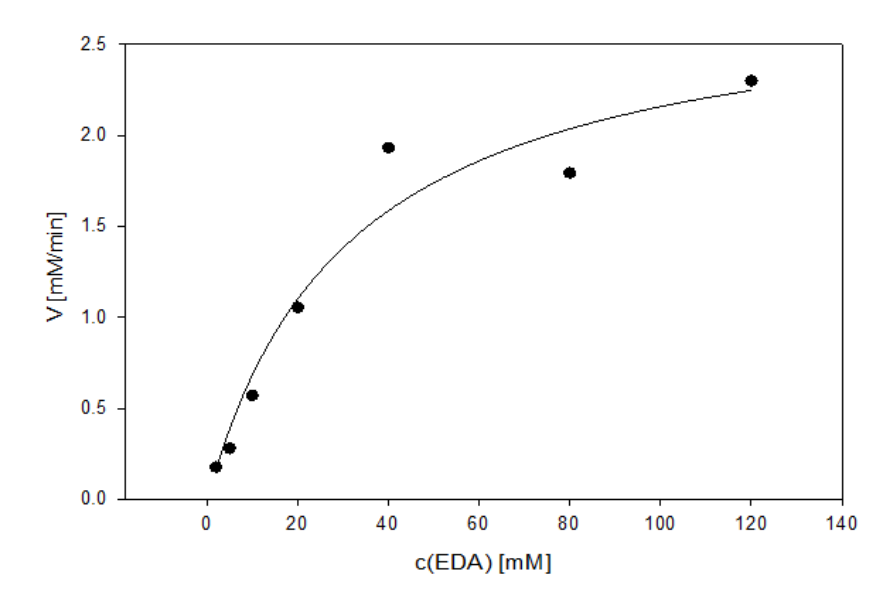


Figure S4. Thermal denaturation curves for (a) Mb(H64V,V68A) and (b) Mb(H64V,V68A)[Fe(Ce6)]. For each protein, a single set of raw data ( $\theta_{MRE}$ ) is shown along with extrapolated signals for folded ( $\theta_{f}$ ) and unfolded ( $\theta_{u}$ ) protein and the fitting curve ( $\theta_{fit}$ ).

# **(a)** Mb(H64V,V68A):



# **(b)** Mb(H64V,V68A)[Fe(Ce6]:



**Figure S5.** Michaelis-Menten curves for cyclopropanation of styrene with EDA in the presence of (a) Mb(H64V,V68A), and (b) Mb(H64V,V68A)[Fe(Ce6] as the catalyst. Reaction conditions: 1  $\mu$ M Mb(H64V,V68A)[Fe(Ce6)] or 10  $\mu$ M Mb(H64V,V68A), 10 mM sodium dithionite, 20 mM styrene, and EDA at varying concentrations (0.5-120 mM) in KPi buffer (50 mM, pH 7.0).

#### **Experimental Procedures**

Reagents. All the chemicals and reagents were purchased from commercial suppliers (Sigma-Aldrich, Alfa Aesar) and used without any further purification, unless otherwise stated. Chlorin e6 was purchased from Frontier Scientific. EDA was purchased from Sigma-Aldrich as 87% m/v solution in dichloromethane. All dry reactions were carried out under argon in oven-dried glassware with magnetic stirring using standard gas-tight syringes, cannulae and septa. Silica gel chromatography purifications were carried out using AMD Silica Gel 60 230-400 mesh. Thin Layer Chromatography (TLC) and preparative TLC were carried out using Merck Millipore TLC silica gel 60 F254 glass plates.

Growth Media. Cell cultures were grown in enriched M9 medium which was prepared as follows. For 1 L, 770 mL deionized H<sub>2</sub>O was added with 200 mL M9 salts (5x) solution, 20 mL glucose (20% v/v), 10 mL casamino acids (20% m/v), 1 mL MgSO<sub>4</sub> (2 M), and 100 μL CaCl<sub>2</sub> (1 M). The M9 salts (5x) solution was prepared by dissolving 15 g Na<sub>2</sub>HPO<sub>4</sub>, 7.5 g K<sub>2</sub>HPO<sub>4</sub>, 0.3 g NaH<sub>2</sub>PO<sub>4</sub>, 0.3 g KH<sub>2</sub>PO<sub>4</sub>, 1.5 g NaCl, 5 g NH<sub>4</sub>Cl in 2 L deionized H<sub>2</sub>O and sterilized by autoclaving. The casamino acids and MgSO<sub>4</sub> solutions were autoclaved separately. The CaCl<sub>2</sub> and glucose stock solutions were sterilized by filtration. Enriched M9 agar plates were prepared by adding 17 g agar to 1 L of enriched M9 media containing all of the aforementioned components at the specified concentrations with the exception of glucose and CaCl<sub>2</sub>, which were added immediately prior to plating. To media and plates, ampicillin was added to a final concentration of 100 mg/L and chloramphenicol was added to a final concentration of 34 mg/L.

In vitro reconstitution and recombinant expression of [Fe(Ce6)]-containing myoglobins. Wild-type Mb, Mb(H64V,V68A), Mb(H64V,V68A,H93A), and Mb(H64V,V68A,H93F) were expressed from pET22-based vectors, whose preparation was described previously. All

proteins contained a C-terminal polyhistidine tag. BL21(DE3) cells were transformed with the pET22-based vector encoding for the appropriate Mb variant and the transformed cells were selected on enriched M9 agar plates containing ampicillin (100 mg L<sup>-1</sup>). Single colonies were used to inoculate 5 mL of enriched M9 media supplemented with ampicillin (100 mg L<sup>-1</sup>), followed by incubation at 37°C with shaking (180 rpm) for 10 to 15 hours. For in vitro reconstitution of the [Fe(Ce6)]-containing myoglobins, the overnight cultures were transferred to 1 L enriched M9 medium containing ampicillin, followed by incubation at 37°C with shaking (180 rpm). At an OD<sub>600</sub> of 1.4, cells were induced with IPTG (final conc.: 0.5 mM) and incubated at 20°C with shaking (180 rpm) for 20 to 24 hours. After harvesting, the cell pellets were resuspended in 20 mL of Ni NTA Lysis Buffer (50 mM KPi, 250 mM NaCl, 10 mM histidine, pH = 8.0) and iron(Cl)-chlorin e6 was added to the cell suspension to a final concentration of 0.05 mM. Cells were lysed by sonication and the cell lysate was clarified by centrifugation (14,000 rpm, 4°C, 30 min).

For the recombinant expression of the [Fe(Ce6)]-containing myoglobins, overnight cultures of C41(DE3) cells containing the appropriate pET22-based expression vector were transferred to 1 L enriched M9 medium containing ampicillin, followed by incubation at 37°C with shaking (180 rpm). At an OD600 of 1.4, cells were condensed (5x) by centrifugation and resuspension in 200 mL of enriched M9 medium. The resulting cell culture was incubated with iron(Cl)-chlorin e6 (final concentration: 30 mg/L) and then induced with IPTG (final conc.: 0.5 mM). Cells were incubated at 20°C with shaking (180 rpm) for 20 to 24 hours. After harvesting, the cell pellets were resuspended in 20 mL of Ni NTA Lysis Buffer (50 mM KPi, 250 mM NaCl, 10 mM histidine, pH = 8.0) and lysed by sonication, and the cell lysate was clarified by centrifugation (14,000 rpm, 4°C, 30 min).

**Protein Purification.** The clarified lysate was transferred to a Ni-NTA column equilibrated with Ni-NTA Lysis Buffer. The resin was washed with 50 mL of Ni-NTA Lysis Buffer and

then 50 mL of Ni-NTA Wash Buffer (50 mM KPi, 250 mM NaCl, 20 mM Histidine, pH = 8.0). Proteins were eluted with Ni-NTA Elution Buffer (50 mM KPi, 250 mM NaCl, 250 mM Histidine, pH = 7.0). After elution from the Ni-NTA column, the protein was buffer exchanged against 50 mM KPi buffer (pH 7.0) using 10 kDa Centricon filters. The concentration of the Mb variants (ferric form) was calculated using an extinction coefficient of  $\varepsilon_{414} = 188 \text{ mM}^{-1} \text{ cm}^{-1}$ , which was determined using the pyridine hemochrome assay<sup>2</sup> with Mb[Fe(Ce6)] and [Fe(Ce6)] as reference.

CD analyses and T<sub>m</sub> determination. Far UV CD spectra (250-190 nm) were obtained using 3 µM solutions of purified Mb variant in 50 mM potassium phosphate buffer (pH 7.0) and recorded at 20°C at a scan rate of 50 nm/min with a bandwidth of 1 nm and an averaging time of 10 seconds per measurement. Visible range CD spectra (500-300 nm) were obtained using a 100 µM solution of purified Mb(H64V,V68A) and a 25 µM solution of purified Mb(H64V,V68A)[Fe(Ce6)] in 50 mM potassium phosphate buffer (pH 7.0). For these experiments, the proteins were reduced with dithionite and exposed to CO for 1 minute prior to recording the CD spectra. Thermal denaturation experiments were carried out using a JASCO J-1100 CD spectrophotometer equipped with variable temperature/wavelength denaturation analysis software and samples of purified Mb variant at 3 µM in 50 mM potassium phosphate buffer (pH 7.0). Thermal denaturation curves were measured by monitoring the change in molar ellipticity at 222 nm ( $\theta_{222}$ ) over a temperature range from 20°C to 100°C. The temperature increase was set to 0.5°C per minute with an equilibration time of 10 seconds. Data integration time for the melt curve was set to 4 seconds with a bandwidth of 1 nm. Linear baselines for the folded ( $\theta_f$ ) and unfolded state ( $\theta_u$ ) were generated using the low temperature ( $\theta_f = m_f T + b_f$ ) and high temperature ( $\theta_u = m_u T + b_u$ ) equations fitted to the experimental data before and after global unfolding, respectively (Figure S2).

Using these equations, the melt data were converted to fraction of folded protein ( $F_f$ ) vs. temperature plots and the resulting curve was fitted to a sigmoidal equation ( $\theta_{fit}$ ) via non-linear regression analysis in SigmaPlot (**Figure 1c**), from which apparent melting temperatures were derived. The reported mean values and standard errors were derived from experiments performed at least in duplicate.

Anaerobic and Aerobic Cyclopropanation Reactions. Reactions with styrene and EDA were carried out as described previously. <sup>1a</sup> Briefly, under standard reaction conditions,  $400 \, \mu L$ -scale reactions were carried out using  $10 \, \mu M$  or  $20 \, \mu M$  Mb variant,  $10 \, mM$  styrene,  $20 \, mM$  EDA and  $10 \, mM$  sodium dithionite. In a typical procedure, a solution containing sodium dithionite ( $100 \, mM$  stock solution) in potassium phosphate buffer ( $50 \, mM$ , pH 7.0) was degassed by bubbling argon into the mixture for  $3 \, min$  in a sealed vial. A buffered solution containing the myoglobin variant was carefully degassed in a similar manner in a separate vial. The two solutions were then mixed together via cannula. Reactions were initiated by addition of  $10 \, \mu L$  of styrene (from a  $0.4 \, M$  stock solution in ethanol), followed by the addition of  $10 \, \mu L$  of EDA (from a  $0.8 \, M$  stock solution in ethanol) with a syringe, and the reaction mixture was stirred for  $12 \, hours$  at room temperature, under positive argon pressure. Aerobic reactions were carried out without degassing the solution with argon and in open reaction vessels. Reactions without reductant were performed in a similar manner without the addition of sodium dithionite. Reactions with the Fe(Ce6) cofactor were performed in a similar manner as mentioned above.

**Whole-cell cyclopropanation reaction.** *E. coli* C41(DE3) cells expressing the Mb(H64V,V68A)[Fe(Ce6)] variant were prepared according to the protocol described above. After harvesting, the cells were suspended in phosphate buffer (KPi pH 7.2) and diluted to an  $OD_{600}$  of 30. The cell suspension was transferred to an open Erlenmeyer flask equipped with a

stir bar and supplemented with 2 mL of a 50 mM p-glucose solution (from a 2 M stock solution). Reaction was initiated by addition of 100 mg of styrene (indicated amount dissolved in 1/100 of total reaction volume of ethanol) in one portion, followed by the addition of 120 µL of EDA (indicated amount dissolved in 1/100 of total reaction volume of ethanol) with a syringe pump over a period of 2 hours at room temperature. Reaction mixtures were stirred at room temperature for 14-16 hours and extracted with ethyl acetate (100 mL x 3). The combined organic layers were dried over sodium sulfate and evaporated under reduced pressure. The crude product was purified by column chromatography (silica gel) with 5-10% diethyl ether/hexanes as the eluent to afford 170 mg of (1*S*,2*S*)-ethyl 2-phenylcyclopropanecarboxylate (5) (93% isolated yield) in 96% *de* and 90% *ee*.

**Product analysis:** Cyclopropanation reactions were analyzed by adding 20 μL of internal standard (benzodioxole, 50 mM in ethanol) to the reaction mixture, followed by extraction with 400 μL of dichloromethane and analysis by gas chromatography (GC). Gas chromatography (GC) analyses were carried out using a Shimadzu GC-2010 gas chromatograph equipped with a FID detector and a Chiral Cyclosil-B column (30 m x 0.25 mm x 0.25 μm film). Separation method for cyclopropanation reaction: 1 μL injection, injector temp.: 200 °C, detector temp: 300 °C. Gradient: column temperature set at 120 °C for 3 min, then to 150 °C at 0.8 °C/min, then to 245 °C at 25 °C/min. Total run time was 46.30 min. Calibration curves for quantification of the cyclopropanation products were constructed using authentic (racemic) standards prepared synthetically or enzymatically as described previously.<sup>3</sup> All measurements were performed at least in duplicate.

**Kinetic (Michaelis-Menten) analyses.** Reactions were carried out on a 400 μL scale using the enzyme at a fixed concentration (Mb(H64V,V68A)[Fe(Ce6)]: 1 μM;

Mb(H64V,V68A)[Fe(ppIX)]: 10  $\mu$ M), 10 mM sodium dithionite, 20 mM styrene, and EDA at varying concentrations (0.5, 1, 2, 5, 10, 20, 40, 80, 120 mM) in KPi buffer (50 mM, pH 7.0). Initial velocity (V) was measured based on the amount of Ethyl 2-phenylcyclopropane-1-carboxylate (5) formed after 30 seconds, at which point the reaction was quenched by the addition of 100  $\mu$ L of 6 M guanidinium hydrochloride in 2 M HCl and immediately extracted with 400  $\mu$ L of dichloromethane containing 20  $\mu$ L of benzodioxole as internal standard. The kinetic parameters  $V_{max}$ ,  $k_{cat}$ , and  $K_{M}$  were obtained by fitting the resulting plot of initial velocity (V) vs. substrate concentrations (c(EDA)) to the Michaelis-Menten equation using SigmaPlot software. Experiments were performed in triplicate and a representative curve is shown in **Figure S5**.

#### **Synthetic Procedures:**

#### Synthesis of Fe(Cl)-chlorin e6 (2).

Chlorin e6 (100 mg) was dissolved in acetone (100 mL) and to the solution (+)-ascorbic acid (360 mg) in acetone (100 mL) and Fe(II)Cl<sub>2</sub>.4H<sub>2</sub>O were added. The reaction mixture was stirred at 60°C for 4 hrs. After cooling to room temperature, the reaction mixture was added with 100 mL dichloromethane and washed with saturated brine solution (3 x 100 mL), then with 100 mL of 0.01 M HCl solution, and then with water (200 mL). The organic layer was dried and evaporated to yield Fe(Cl) chlorin e6 as a dark green powder (113 mg, 96%). All the processes were done in the dark and under argon atmosphere. LC-MS: *m/z* ([M – Cl]<sup>+</sup>) calc. 650.5; obs. 650.0. UV-Vis (ε M<sup>-1</sup> cm<sup>-1</sup>): 395 nm (33,840), 603 nm (5,900), 684 nm (7,700).

For NMR characterization, 20 mg of the complex were dissolved in a minimal amount of MeOH (0.5-1 mL) and diluted with 3 mL 0.1 M sodium phosphate buffer (pH 5). Slow acidification with 0.5 M HCl resulted in precipitation of a dark green solid, which was centrifuged and the light green supernatant decanted. The precipitate was washed twice with 6 mL water and dried *in vacuo*. Fe(Cl)-chlorin e6 was converted into the corresponding biscyano complex according to a modified procedure for porphyrin iron(III) chlorides.<sup>4</sup> The complex was dissolved in MeOH- $d_4$  (0.05 M solution) and subsequently treated with 5

equivalents of potassium cyanide. The mixture was incubated for 30 min, sonicated and centrifuged prior to NMR analysis. The NMR spectrum showed the occurrence of ligand exchange with the solvent to give two Fe(CN)(MeOH)-chlorin e6 complexes, i.e., with the methanol ligand residing on either side of the chlorin e6 plane, in addition to the *bis*-cyano complex (Fe(CN)<sub>2</sub>-chlorin e6). Indicative of the mixed ligand complexes were two sets of downfield signals (-0.33/-0.12 ppm and -4.07/-4.20 ppm, each with 3:1 rel. int.), which were attributed to the metal-bound methanol from the two cyano/methanol complexes. This assignment was confirmed by H/D exchange experiments, which showed disappearance of the signals at -0.33 and -4.20 ppm upon addition of D<sub>2</sub>O (see insert in <sup>1</sup>H NMR spectrum). The ligand-exchanged complexes likely account for the downfield signals (>180 ppm) observed in the <sup>13</sup>C NMR spectrum.

L = CN or MeOH

 3H, C*H*<sub>3</sub>OH), -0.33 (br, 1H, CH<sub>3</sub>O*H*), -4.07 (s, 3H, C*H*<sub>3</sub>OH), -4.20 (br, 1H, CH<sub>3</sub>O*H*). <sup>13</sup>C NMR (125 MHz, MeOH-*d4*) δ 182.2, 181.6, 180.4, 177.7, 170.9, 169.6, 159.8, 153.6, 150.4, 144.9, 138.3, 137.1, 136.9, 134.6, 134.2, 133.5, 132.5, 130.8, 130.1, 121.4, 108.9, 100.0, 99.0, 95.0, 55.6, 42.6, 36.5, 32.9, 24.0, 20.6, 20.4, 18.1, 13.4, 12.2, 12.1, 11.3, 4.9.

**Synthesis of olefin substrates and cyclopropanation products.** Compound **16a** and **17a** were synthesized as described in Bajaj *et al.*.<sup>3</sup> Authentic standards for **5** and **6b-17b** were prepared as described previously. <sup>1a,3</sup>

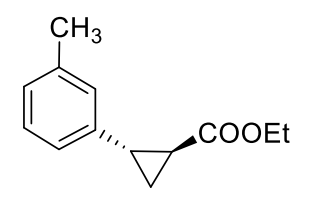
#### **Ethyl 2-phenylcyclopropane-1-carboxylate (5):**

GC-MS m/z (% relative intensity): 190(29.5), 144(28.3), 135(20.7), 117(100), 107(7.3);  $^{1}$ H NMR (CDCl<sub>3</sub>, 400 MHz):  $\delta$  7.34-7.28 (m, 2H), 7.23-7.20 (m, 1H), 7.11 (d, J = 7.2 Hz, 2H), 4.19 (q, J = 7.2 Hz, 2H), 2.56-2.51 (m, 1H), 1.94-1.90 (m, 1H), 1.64-1.59 (m, 1H), 1.35-1.30 (4H) ppm;  $^{13}$ C NMR (CDCl<sub>3</sub>, 100 MHz):  $\delta$  173.2, 140.0, 128.3, 126.3, 126.0, 60.6, 26.1, 24.1, 17.0, 14.2 ppm.

#### Ethyl 2-(o-tolyl)cyclopropane-1-carboxylate (6b):

GC-MS m/z (% relative intensity): 204(29.13), 158(16.7), 147(16.7), 131(100), 91(28.30).  $^{1}$ H NMR (CDCl<sub>3</sub>, 400 MHz):  $\delta$  7.16 (m, 3H), 7-01-6.99 (m, 1H), 4.23 (q, J = 7.6 Hz, 2H), 2.55-2.49 (m, 1H), 2.38 (s, 3H), 1.82-1.76 (m, 1H), 1.60-1.55 (m, 1H), 1.31-1.28 (m, 4H) ppm,  $^{13}$ C NMR (CDCl<sub>3</sub>, 100 MHz):  $\delta$  173.8, 138.0, 137.8, 129.8, 126.7, 125.8, 60.6, 24.6, 22.3, 19.5, 15.3, 14.3 ppm.

#### Ethyl 2-(m-tolyl)cyclopropane-1-carboxylate (7b):



GC-MS m/z (% relative intensity): 204(20.9), 158(16.1), 147(13.7), 131(100), 115(21.2).  $^{1}$ H NMR (CDCl<sub>3</sub>, 400 MHz):  $\delta$  7.19-7.16 (m, 1H), 7.03-7.01 (m, 1H), 6.93-6.89 (m, 2H), 4.20 (q, J = 6.8 Hz, 2H), 2.50-2.49 (m, 1H), 2.33 (s, 3H), 1.91-1.88 (m, 1H), 1.60-1.57 (m, 1H), 1.31-1.27 (m, 4H) ppm,  $^{13}$ C NMR (CDCl<sub>3</sub>, 100 MHz):  $\delta$  173.4, 140.0, 138.0, 128.3, 127.2, 127.0, 123.1 60.6, 26.1, 24.1, 21.3, 16.9, 14.3 ppm.

# Ethyl 2-(p-tolyl)cyclopropane-1-carboxylate (8b):

GC-MS m/z (% relative intensity): 204(28.4), 158(19.7), 147(21.1), 131(100), 91(28.1);  $^{1}$ H NMR (CDCl<sub>3</sub>, 400 MHz):  $\delta$  7.11 (d, J = 7.6 Hz, 2H), 7.01 (d, J = 7.6 Hz, 2H), 4.21 (q, J = 7.2 Hz, 2H), 2.53-2.48 (m, 1H), 2.32 (s, 3H), 1.90-1.85 (m, 1H), 1.61-1.56 (m, 1H), 1.31-1.27 (m, 4H) ppm,  $^{13}$ C NMR (CDCl<sub>3</sub>, 100 MHz):  $\delta$  173.5, 137.0, 136.0, 129.1, 126.1, 60.6, 25.9, 24.0, 20.9, 16.9, 14.2 ppm.

#### Ethyl 2-(4-chlorophenyl)cyclopropane-1-carboxylate (9b):

Following the standard procedure, yield = 82%, GC-MS m/z (% relative intensity): 224(38.9), 178(20.9), 151(100), 115(98.9), 89(14.9), *E-isomers*: colorless liquid, <sup>1</sup>H NMR (CDCl<sub>3</sub>, 400 MHz):  $\delta$  7.24 (d, J = 7.6 Hz, 2H), 7.02 (d, J = 7.2 Hz, 2H), 4.19 (q, J = 6.8 Hz, 2H), 2.50-2.45 (m, 1H), 1.87-1.83 (m, 1H), 1.61-1.56 (m, 1H), 1.29-1.23 (m, 4H) ppm, <sup>13</sup>C NMR (CDCl<sub>3</sub>, 100 MHz):  $\delta$  173.1, 138.6, 132.1, 128.5, 127.5, 60.8, 25.4, 24.1, 16.9, 14.2 ppm.

#### Ethyl 2-(4-methoxyphenyl)cyclopropane-1-carboxylate (10b):

GC-MS m/z (% relative intensity): 220(41.8), 191(14.5), 147(100), 91(32.6). <sup>1</sup>H NMR (CDCl<sub>3</sub>, 400 MHz):  $\delta$  7.03(d, J = 8.4 Hz, 2H), 6.82 (d, J = 8.4 Hz, 2H), 4.18 (q, J = 7.2 Hz, 2H), 3.76 (s, 3H), 2.49-2.45 (m, 1H), 1.83-1.79 (m, 1H), 1.56-1.52 (m, 1H), 1.32-1.21 (m, 4H), <sup>13</sup>C NMR (CDCl<sub>3</sub>, 100 MHz):  $\delta$  173.5, 158.3, 132.1, 127.5, 113.9, 60.6, 55.2, 25.6, 23.8, 16.7, 14.2 ppm.

#### Ethyl 2-(3,4-difluorophenyl)cyclopropane-1-carboxylate (11b):

GC-MS m/z (% relative intensity): 226(56.1), 198(18.3), 181(25.7), 153(100), 133(53.3), 125(39.1), 101(6.8);  $^{1}$ H NMR (CDCl<sub>3</sub>, 400 MHz):  $\delta$  7.04-6.98 (m, 1H), 6.87-6.78 (m, 2H), 4.13 (q, J = 7.2 Hz, 2H), 2.46-2.41 (m, 1 H), 1.82-1.78 (m, 1H), 1.57-1.52 (m, 1H), 1.24 (t, J = 6.8 Hz, 3H), 1.21-1.17 (m, 1H) ppm,  $^{13}$ C NMR (CDCl<sub>3</sub>, 100 MHz):  $\delta$  172.7, 151.4, 151.3, 150.2, 150.1, 148.9, 148.8, 147.8, 147.7, 137.0, 122.2, 177.1, 116.9, 115.1, 114.9, 60.7, 24.9, 23.9, 16.7, 14.1 ppm.

#### Ethyl 2-methyl-2-phenylcyclopropane-1-carboxylate (12b):

GC-MS m/z (% relative intensity): 204(4.18), 175(9.7), 159(15.19), 147(13.9), 131(100), 91(41.1).  $^{1}$ H NMR (CDCl<sub>3</sub>, 400 MHz):  $\delta$  7.30 (m, 4H), 7.22-7.20 (m, 1H), 4.23 (q, J = 6.2 Hz, 2H), 1.99-1.96 (m, 1H), 1.54 (s, 3H), 1.46-1.40 (m, 2H), 1.32-1.29 (m, 3H) ppm,  $^{13}$ C NMR (CDCl<sub>3</sub>, 100 MHz):  $\delta$  172.1, 145.9, 128.4, 127.3, 126.4, 60.4, 30.5, 27.8, 20.7, 19.6, 14.4 ppm.

#### Ethyl 2-(naphthalen-1-yl) cyclopropane-1-carboxylate (13b):

GC-MS m/z (% relative intensity): 240(34.3), 167(100), 152(54.1), 115(7.2); <sup>1</sup>H NMR (CDCl<sub>3</sub>, 400 MHz):  $\delta$  8.22 (d, J = 8.4 Hz, 1H), 7.88 (d, J = 8.0 Hz, 1H), 7.77 (d, J = 8.0 Hz, 1H), 7.61-7.52 (m, 2H), 7.41 (t, J = 8.0 Hz, 1H), 7.29 (d, J = 8 Hz, 1H), 4.32-4.26 (m, 2H), 3.06-3.01 (m, 1H), 1.99-1.95 (m, 1H), 1.77-1.72 (m, 1H), 1.48-1.43 (m, 1H), 1.37 (t, J = 7.2 Hz, 3H) ppm; <sup>13</sup>C NMR (CDCl<sub>3</sub>, 100 MHz):  $\delta$  174.0, 138.1, 135.9, 133.7, 137.7, 133.1, 128.7, 127.7, 126.4, 126.0, 125.5, 124.2, 60.9, 24.2, 22.4, 15.6, 14.5 ppm.

# Ethyl 2-methyl-2-(thiophen-3-yl)cyclopropane-1-carboxylate (14b):

GC-MS m/z (% relative intensity): 210(24.6), 165(14.6), 137(100), 103(6.9); <sup>1</sup>H NMR (CDCl<sub>3</sub>, 400 MHz):  $\delta$  7.22-7.20 (m, 1H), 6.98-6.97 (m, 1H), 6.84 (d, J = 4.8 Hz, 1H), 1.94 (dd, J = 8.4, 6.4 Hz, 1H), 1.54 (s, 3H), 1.46-1.44 (m, 1H), 1.39-1.36 (m, 1H), 1.24 (t, J = 7.2 Hz, 3H) ppm; <sup>13</sup>C NMR (CDCl<sub>3</sub>, 100 MHz):  $\delta$  171.5, 146.9, 125.7, 125.3, 119.3, 60.4, 29.1, 25.9, 22.1, 17.8, 14.2 ppm.

#### Ethyl 2-methyl-2-(pyridin-2-yl)cyclopropane-1-carboxylate (15b):

GC-MS m/z (% relative intensity): 205(25.1), 176(43.4), 132(100), 117(68.7), 104(9.2);  $^{1}$ H NMR (CDCl<sub>3</sub>, 400 MHz):  $\delta$  68.48 (d, J = 4.0 Hz, 1H), 7.62-7.59 (m, 1H), 7.37 (d, J = 8.0 Hz, 1H), 7.08 (dd, J = 8.0, 4.0 Hz 1H), 4.19-4.13 (m, 2H), 2.39-2.37(m, 1H), 1.80-1.78 (m, 1H), 1.63 (s, 3H), 1.49-1.47 (m, 1H), 1.26 (t, J = 8.0 Hz, 3H) ppm;  $^{13}$ C NMR (CDCl<sub>3</sub>, 125 MHz):  $\delta$  171.9, 162.4, 149.0, 136.1, 120.9, 120.2, 60.5, 29.9, 29.3, 22.5, 15.7, 14.4 ppm.

#### Ethyl 2-methyl-2-(6-(trifluoromethyl)pyridin-3-yl)cyclopropane-1-carboxylate (16b):

GC-MS m/z (% relative intensity): 273(20.8), 244(76.4), 228(43.3), 200(100), 180(68.3), 130(20.7);  $^{1}$ H NMR (CDCl<sub>3</sub>, 500 MHz):  $\delta$  8.63 (d, J =1, Hz, 1H), 7.74 (dd, J = 8.5, 2.0 Hz, 1H), 7.59 (d, J = 8.0 Hz, 1H), 4.21-4.15 (m, 2H), 1.96 (dd, J = 8.5, 6.0 Hz, 1H), 1.52 (s, 3H), 1.44 (dd, J = 8.5, 5.5 Hz, 3H), 1.27 (t, J = 7.5 Hz, 3H) ppm;  $^{13}$ C NMR (CDCl<sub>3</sub>, 125 MHz):  $\delta$  171.1, 149.3, 146.7, 146.4, 146.1, 145.9, 144.4, 136.1, 124.8, 122.6, 120.4, 120.2, 120.1, 60.9, 27.7, 20.3, 19.1, 14.3 ppm.

# Ethyl 2-(2,3-dihydrobenzofuran-4-yl)cyclopropane-1-carboxylate (17b):

GC-MS m/z (% relative intensity): 232(100), 159(90.1), 144(68.9), 132(70.2), 115(43.5), 101(16.7);  $^{1}$ H NMR (CDCl<sub>3</sub>, 500 MHz):  $\delta$  7.04 (t, J = 8.0 Hz, 1H), 6.65 (d, J = 8.0 Hz, 1H), 6.41 (d, J = 8.0 Hz, 1H), 4.59 (t, J = 8.4 Hz, 2H), 4.19 (q, J = 7.2 Hz, 2H), 3.24 (t, J = 8.4 Hz, 2H), 32.44-2.39 (m, 1H), 1.93-1.88 (m, 1H), 1.60-1.56 (m, 1H), 1.32 (t, J = 4.4 Hz, 3H) ppm;  $^{13}$ C NMR (CDCl<sub>3</sub>, 100 MHz):  $\delta$  173.4, 159.7, 136.5, 128.1, 126.4, 116.0, 107.4, 70.9, 60.6, 28.4, 23.8, 22.7, 15.9, 14.1 ppm.

# References

- (1) (a) Bordeaux, M.; Tyagi, V.; Fasan, R. Angew. Chem. Int. Ed. 2015, 54, 1744; (b) Sreenilayam, G.; Moore, E. J.; Steck, V.; Fasan, R. Adv. Synth. Cat. 2017, 359, 2076.
- (2) Berry, E. A.; Trumpower, B. L. Analyt. Biochem. 1987, 161, 1.
- (3) Bajaj, P.; Sreenilayam, G.; Tyagi, V.; Fasan, R. Angew. Chem. Int. Ed. 2016, 55, 16110.
- (4) La Mar, G. N.; Viscio, D. B.; Smith, K. M.; Caughey, W.; Smith, M. L. J. Am. Chem. Soc. 1978, 100, 8085.

<sup>1</sup>H NMR of Fe(CN)<sub>2</sub>-chlorin e6 complex in MeOH- $d_4$ . Insert: Upfield region after addition of D<sub>2</sub>O (30 μL). \* = grease -0.115 .194 3.235 2.571 2.357 2.218 1.769 1.755 99.712 99.0011 99.0 0.114 986 3 ppm 3.11

3.48 3.35 3.35 3.13 1.66 1.70 1.70 7.82

5

1.17

1.19

12

11

10

1.00

9

8

96.0

0

-4 ppm

<sup>13</sup>C NMR of Fe(CN)<sub>2</sub>-chlorin e6 complex in MeOH- $d_4$ . \* = grease; # = MeOH.

